Oscillatory exchange coupling in Fe/Cr multilayers

M. D. Stiles

Electron Physics Group, National Institute of Standards and Technology, Gaithersburg, Maryland 20899

(Received 3 May 1996)

First-principles calculations of the reflection probabilities for Fermi-surface electrons at Cr/Fe interfaces are used to compute the strength of the oscillatory exchange coupling in Cr/Fe multilayers. These calculations show that critical spanning vectors across the N-centered ellipsoids of the Cr Fermi surface cause the long-period coupling for (001), (110), and (211) interfaces. The periods of these spanning vectors, when extracted from the experimental Fermi surface, agree with experimentally measured periods. [S0163-1829(96)07544-3]

I. INTRODUCTION

Fe/Cr multilayers were the first systems to exhibit exchange coupling,[1] giant magnetoresistance,[2] oscillatory exchange coupling,[3] and short-period oscillatory exchange coupling.[4–6] In spite of this early start and a large amount of theoretical and experimental efforts,[7,8] there are still many aspects of these systems that are unknown. In this paper I focus on the oscillatory exchange coupling, and in particular on the long-period component.

For (001)-oriented films, at least two oscillatory coupling periods are observed.[9] When the films are grown by sputtering, or at low temperatures, the coupling oscillates with a long period, of approximately 12 ML. When the multilayer is grown at elevated temperatures on high quality substrates, the oscillatory coupling has a short period of approximately 2.1 ML. Whether or not the short-period oscillations are observed depends on the roughness of the interfaces. If the interfaces are rough on a lateral length scale much shorter than the length over which the Fe layers can change magnetization direction, the interlayer coupling is frustrated in some regions. The coupling over large regions becomes the average of the coupling for several thicknesses. As a result, the short-period oscillation is weakened much more than the long-period oscillation.[10] Comparing roughness measurements by scanning tunneling microscopy[9] with coupling measurements for different growth temperatures bears out this expectation.

It is generally accepted that short-period oscillatory coupling arises from the ''nested'' parts of the Cr Fermi surface (see the spanning vectors labeled ''A'' in Fig. 1). ''Nested'' refers to regions of the Fermi surface that are parallel to each other over an extended area in reciprocal space.[11] This nesting produces the spin-density-wave antiferromagnetism found in bulk Cr, which has a Néel temperature of about room temperature. The nested parts of the Fermi surface are also believed to cause the strong short-period oscillation in the exchange coupling, although the best description of this coupling is not known. One description is that the Cr is antiferromagnetic, possibly stabilized in this state by the presence of Fe. Another description is that Cr responds paramagnetically to the presence of the Fe. In this description, the Fe excites a spin-density wave in Cr that is dominated by the response of the nested regions of the Fermi surface. In fact, it can be quite difficult to find differences between the two

descriptions that are not purely semantic. One such difference is that when Cr is in its antiferromagnetic state, a gap opens at the Fermi level, and parts of the Fermi surface disappear. As a consequence, there are anomalies in the transport properties as the temperature is raised or lowered through the Néel temperature. While such anomalies have not been found for samples showing short-period oscillations in the coupling, measurements[12] indicate that in some, but not necessarily all, of the samples in which the long-period oscillation is observed, the Cr is not antiferromagnetic.

Films grown with a (211) orientation also exhibit a long-period oscillation in the exchange coupling,[13] 1.8 nm, which is the same as that found for the similar (001)-oriented films. In addition, polycrystalline films with a (110) texture also show the same long-period.[3] The common long-period for all three orientations suggests that there may be a common origin to coupling in all three cases. A long-period oscillation is also found in all calculations that include the Cr Fermi surface, whether they be Ruderman-Kittel-Kasoya-Yosida calculations,[10] or calculations based on the local-density approximation.[14–17] In spite of all this work, the origin of the long-period oscillation has not been definitively identified.

In Sec. II of this paper, I present calculations of the probabilities for electrons at the Fermi surface of Cr to reflect from Cr/Fe interfaces. These reflection probabilities are used in Sec. III to compute the strength of the oscillatory exchange coupling associated with critical spanning vectors of the Cr Fermi surface. The results show that for all three interface orientations the long-period oscillation is due to critical spanning vectors of the Cr Fermi surface across the ellipsoids centered at the N point of the Brillouin zone [for those responsible for the coupling in (001)-oriented multilayers, see the spanning vectors labeled ''C'' in Fig. 1]. The calculations are then used to discuss the other proposed models for the long-period oscillations in Sec. IV. The results are good agreement with the results of Tsetseris, Lee, and Chang[18] who reached the same conclusions based on similar calculations using a tight-binding description of the band structures.

II. REFLECTION PROBABILITIES

Spin-dependent reflection probabilities facilitate the understanding of many properties of magnetic multilayers.[19] For example, the electronic states of arbitrary multilayers,
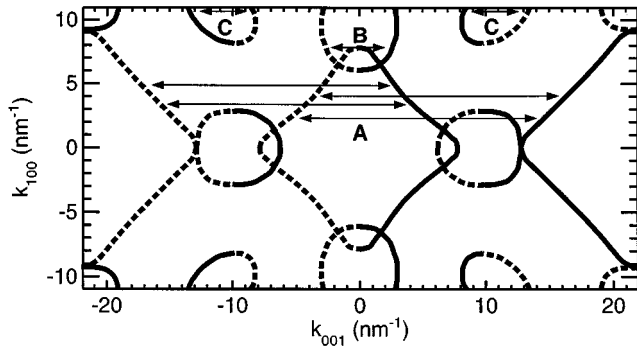
FIG. 1. Slice through Cr Fermi surface for an interface in the (001) direction. The parts of the Fermi surface with states moving toward (away from) the interface are shown as solid (dashed) lines. Spanning vectors associated with several parts of the surface are shown as arrows and labeled. Spanning vectors in the nesting region are labeled A, a spanning vector close to the lens is labeled B, and the critical spanning vectors of the N-centered ellipsoid are labeled C.

including superlattices, can be constructed from the bulk band structures and the reflection amplitudes, provided the interfaces are not too close together.[20] Such states include quantum-well states that can be observed in photoemission experiments[21,22] in systems with a thin layer on a substrate, when there is strong reflection from the interfaces. Reflection from interfaces can have a strong impact on transport in magnetic multilayers, giving a resistance for perpendicular transport and a channeling effect for parallel transport. Finally the spin-dependent reflection amplitudes determine the strength of the oscillatory exchange coupling. In Sec. III, I use the spin-dependent reflection amplitudes at certain critical points on the Fermi surface to determine the strength and origin of the oscillatory exchange coupling.

The reflection probabilities are found by computing the time-independent scattering states for a system with a single interface between semi-infinite Cr and Fe. The interfaces are assumed to be defect free and coherent; that is, both materials have the same in-plane lattice constant. Thus the momentum parallel to the interface is conserved during transmission and reflection. The calculation[23] of the time-independent scattering states starts by breaking space up into layers. The potential is computed for each layer from a bulk electronic structure calculation (a linearized-augmented-plane-wave implementation of the local-spin-density approximation). Generalized Bloch states for a layer are computed from the potential in the layer. The electron scattering states are constructed by matching the generalized Bloch states for the two materials across the interface. The boundary conditions for the scattering states, applied far from the interface, are that there be a single incident bulk Bloch state and possibly several reflected and transmitted bulk Bloch states. The amplitudes of the reflected and transmitted states give the reflection and transmission amplitudes directly.

In these calculations, both Fe and Cr are in the body-centered-cubic structure using the bulk Fe lattice constant for both materials. No significant differences are found in calculations for (001)-oriented interfaces using body-centered-tetragonal Cr, in which the tetragonal distortion is based on the in-plane lattice constant of Fe and the bulk elastic con-
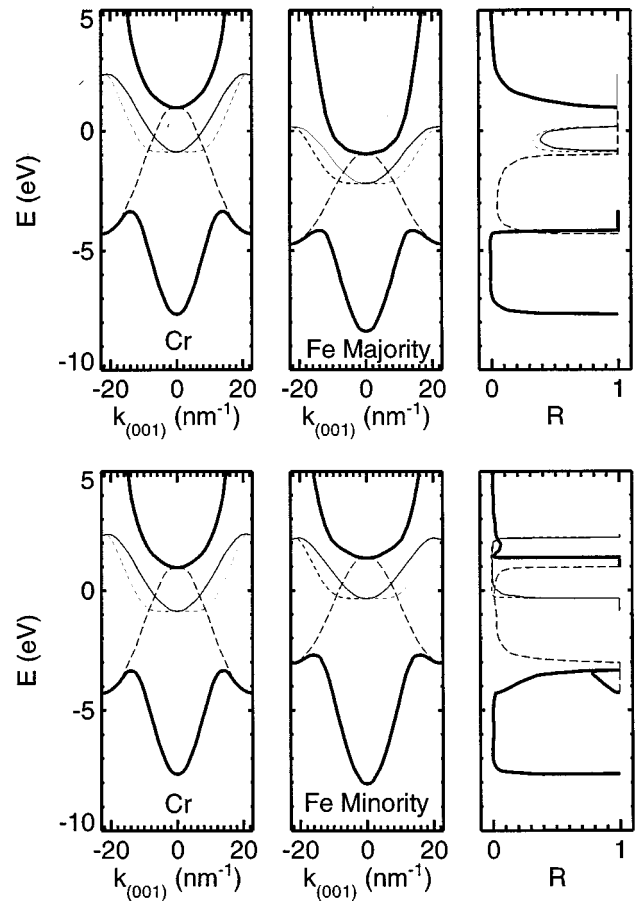

FIG. 2. Spin-dependent reflection probabilities for Cr electrons at $\bar{\Gamma}$ from Cr/Fe interfaces. The two left panels show the (spin-independent) band energies for Cr. The two middle panels show the band energies for the majority (top) and minority (bottom) for Fe. The two right columns show the reflection probability (on the x axis) for each of the Cr states from the majority (top) and minority (bottom) spin systems of the Fe. Different line types are used for the different symmetries of the states.

stants of Cr. The Fe is ferromagnetic and the Cr is paramagnetic. Although the magnetic state of Cr next to Fe as a function of temperature is not known, measurements[12] show that, for some samples at least, the long-period oscillation is found in multilayers in which the Cr is *not* in the antiferromagnetic state. Thus the origin of the long-period oscillation should not depend on the presence of antiferromagnetic order.

In the ferromagnetic state of Fe, approximately one electron is transferred from the minority-spin system to the majority-spin system. Roughly speaking, this leads to a shift of the d bands relative to each other for each spin. The minority band structure becomes very similar to the band structure of the material two places to the left in the Periodic Table, which happens to be Cr. This effect is illustrated in Fig. 2, which shows the band structures of Cr and Fe along the Δ line in the bulk Brillouin zone.

For (001) interfaces, one Δ line projects onto the zone center $\bar{\Gamma}$. Figure 2 shows the probability for each state along this line in Cr to reflect from the interface with Fe, depending on the spin of the electron. These results illustrate general features of reflection probabilities. First, only states that
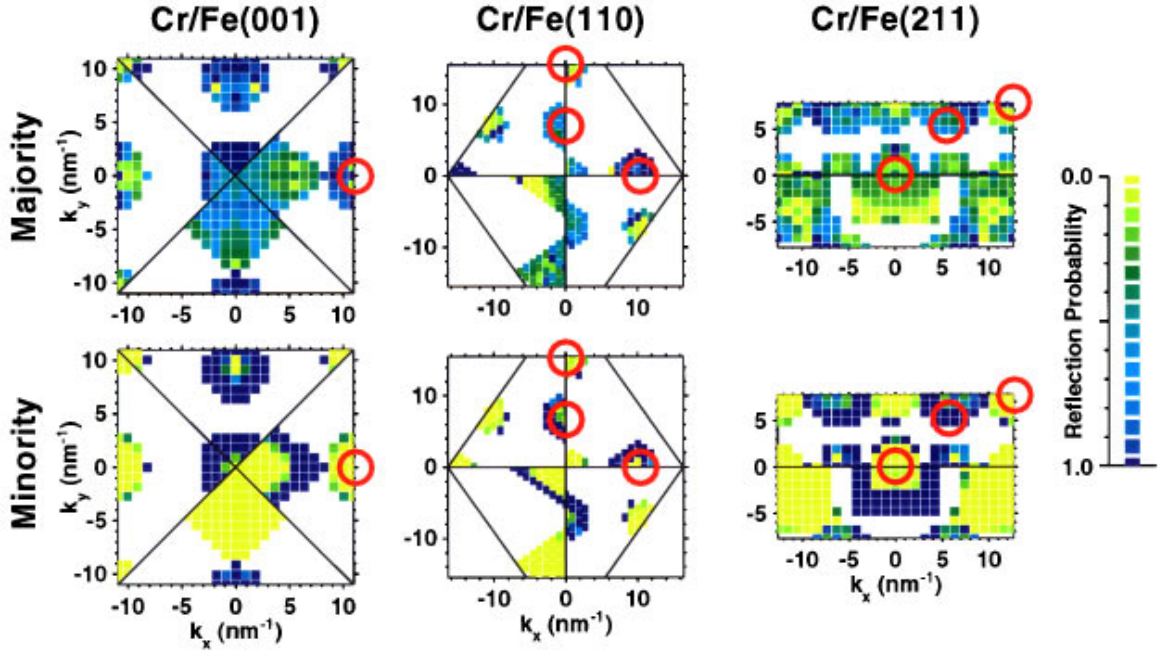
FIG. 3. Spin-dependent reflection probabilities for Cr Fermi-surface electrons from Cr/Fe interfaces. The reflection probabilities are shown for various points on the Fermi surface projected onto the interface Brillouin zones. The color scale for the reflection probability is at the right. The top (bottom) panels show the probabilities for Cr electrons to reflect from the majority (minority) states. The Cr Fermi surface has several sheets, each of which is only shown in a fraction of the Brillouin zone, as otherwise, the sheets would overlap each other. Red circles indicate the location of critical spanning vectors that give rise to strong long-period oscillations, as given in Table II.
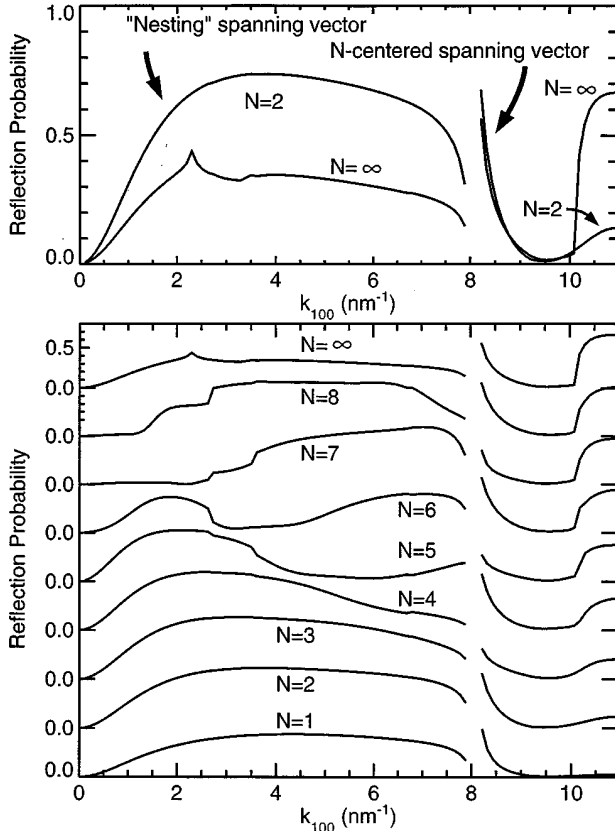

FIG. 4. State-to-state reflection probabilities for selected Cr electrons from Fe layers of finite thickness, N layers, embedded in bulk Cr. The bottom panel shows the reflection probabilities both for the states along $\bar{\Delta}$ associated with the nesting of the Fermi surface, and for the states at the N-centered ellipsoids. The top panel shows the same results for just a two-layer-thick Fe film and bulk Fe.
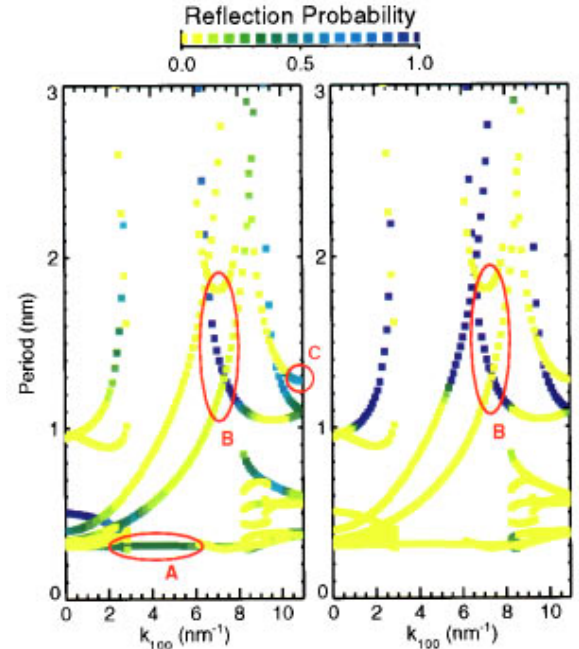

FIG. 5. State-to-state reflection probabilities for Cr electrons from Cr/Fe interfaces. The left and right panels shows the period associated with each spanning vector. In addition, the periods are plotted with a color scale (shown at the top) that gives the probabilities for the two states to reflect into each other when reflecting from Cr/Fe interfaces. The left (right) panel gives these results for the majority (minority) spins. Regions that contain the results for the spanning vectors indicated on the Fermi surface in Fig. 1 are circled and labeled.

TABLE I. Reflection probabilities averaged over the Fermi surface for majority, ↑, and minority, ↓, electrons.

	$Cr \rightarrow Fe_{\downarrow}$	$Fe_{\downarrow} \rightarrow Cr$	$Cr \rightarrow Fe_{\uparrow}$	$Fe_{\uparrow} \rightarrow Cr$
Cr/Fe(001)	0.42	0.18	0.64	0.59
Cr/Fe(110)	0.41	0.16	0.52	0.61
Cr/Fe(211)	0.41	0.18	0.41	0.61

have the same symmetry with respect to the interface can couple to each other. The (001) interface has four mirror planes and a fourfold rotation axis, so that, at the zone center, there are five different possible symmetries for bands derived from s, p, and d states. States of different symmetries are shown with different line types. For a state of a particular symmetry, the reflection is complete if there are no states with the same symmetry in the other material. Complete reflection is found in the vertical line segments in Fig. 2. Second, as a function of energy, the reflection probability decreases from 1 as the square root of the energy relative to each threshold. These thresholds occur at band extrema for states of a particular symmetry. In Fig. 2, each time the reflection probability decreases from 1, it does so with square-root behavior as a function of energy. Finally, these results show that, for materials that are as similar as these, away from such thresholds the reflection probabilities are small.

For the states near the Fermi level, the reflection is weak for minority electrons, because there are states of the same symmetry, but strong for the majority electrons, because there are either no states of the same symmetry, or the states are close to a threshold. At other parallel wave vectors, the symmetry of the states is reduced because symmetry operations that do not map the wave vector into itself do not apply to the states. However, vestiges of the symmetry remain, and influence the reflection throughout the interface Brillouin zone.

For three interface orientations, Fig. 3 shows the reflection probability of Fermi-surface electrons in the entire interface Brillouin zone. For minority electrons, the reflection is weak for most of the electrons, because the Fe minority Fermi surface is very similar to that of Cr. However, the Fermi surfaces are of slightly different sizes, so some electrons reflect completely. The averages over the Fermi surface, in Table I, show that this behavior is only weakly dependent on the interface orientation. For the majority electrons, the reflection is much more complicated, and depends more strongly on interface orientation. The symmetries of the states on the Fermi surfaces are not as well matched between the majority states of Fe and the states of Cr. Thus, for interfaces of higher symmetry, the reflection tends to be larger. The (001) interface has a fourfold axis and four mirror planes, the (110) interface has a twofold axis and two mirror planes, and the (211) interface has a single mirror plane.

III. OSCILLATORY EXCHANGE COUPLING

Most analyses of long-period oscillatory coupling relate the origin of the coupling to critical spanning vectors of the Cr Fermi surfaces, as is suggested by general models of oscillatory exchange coupling.[24,25] The oscillatory exchange coupling strength depends on the spin-dependent reflection amplitudes at these critical points on the Fermi surface.[26,27] In Sec. II, the reflection probabilities were computed for two semi-infinite layers. These results can be used to investigate the coupling strength for two semi-infinite Fe layers surrounding a finite Cr slab, provided the Cr slab is not too thin. For large Cr thicknesses d, the coupling becomes a sum of contributions that oscillate as a function of thickness,

$$J(d) = \sum_{\alpha} \frac{J^{\alpha}}{d^2} \sin(q_{\perp}^{\alpha} d + \phi^{\alpha}). \quad (1)$$

Here the sum over α is the sum over all critical points of the Fermi surface. The critical points are certain points on the Fermi surface where two sheets are parallel to each other at a given wave vector parallel to the interface. In addition, the state on one sheet must be moving toward the interface, and that on the other must be moving away from it. Analyses of the Cr Fermi surface, as calculated in the local-density approximation, find many critical spanning vectors due to the complexity of the Fermi surface.[27,28] The coupling strength for each of these contributions is of the form

$$\frac{J^{\alpha}}{d^2} \sin(q_{\perp}^{\alpha} d + \phi^{\alpha}) = \frac{\hbar v_{\perp}^{\alpha} \kappa^{\alpha}}{4\pi^2 d^2} \mathrm{Im}[\Delta r_A^{\alpha} \Delta r_B^{\alpha} e^{iq_{\perp}^{\alpha} d} e^{i\chi^{\alpha}}], \quad (2)$$

where $v_{\perp}^{\alpha}$ is the component of the effective group velocity in the interface direction, κ^{α} is the radius of curvature of the Fermi surface, $\Delta r_{A(B)}^{\alpha}$ is the spin difference in the state-to-state reflection amplitude for the left (right) interface, $q_{\perp}^{\alpha}$ is the critical spanning vector, which determines the period of the oscillation, $L^{\alpha} = 2\pi/q_{\perp}^{\alpha}$, χ^{α} is a phase from the type of critical point (maximum, minimum, saddle point), and ϕ^{α} is the resulting phase (the reflection amplitudes are complex.) State-to-state reflection refers to the process of reflecting from one state into another particular state, the two states being Fermi-surface states at the critical point. When the coupling strengths are computed for each of the critical spanning vectors, most of them are found to be quite weak.

In regions where the sheets of the Fermi surface are parallel over an extended part of the Fermi surface, not just at a point, the behavior is more complicated. This is the case for the ''nested'' region of the Cr Fermi surface that causes the short-period coupling. Here, the coupling is expected to decrease like $1/d$, and the strength cannot be simply related to the spin-dependent reflection at one critical point.

To find the origin of the long-period oscillatory coupling for these three orientations, I carried out a systematic search of the Fermi surface for all of the critical spanning vectors.[27] Then, to determine the origin of the long-period oscillation, I computed the coupling strength for each of the critical points that had a period of greater than 0.9 nm. The results for critical points with substantial amplitude are given in Table II. The location of these critical spanning vectors on the Fermi surface is shown in Fig. 3. For each orientation the strongest long-period oscillation is associated with the ellipsoids centered at the N point of the bulk Brillouin zone. For the (001) interface, this critical point is the only one with significant strength.

The periods found in this calculation differ significantly from the experimentally measured periods. However, this

disagreement is due to inaccuracies of the local-density approximation. For the N-centered ellipsoids, de Haas–van Alphen measurements[11,29] give an accurate determination of that part of the Fermi surface. Using these measurements to predict the periods for each of the critical points, as is shown in Table II, the results are in good agreement with the measured periods for all three orientations. These same inaccuracies will affect the calculated coupling strengths, as is the case in all calculations based on the local-density approximation. However, they should not affect the qualitative conclusion that origin of the long-period coupling is coupling across the N-centered ellipsoids. In all cases of strong coupling for the N-centered ellipsoids, the strong reflection results from the symmetries of the states.

Koelling[28] makes an additional argument for why the N-centered ellipsoids could be responsible for the coupling. Most of the Cr Fermi surface consists of states that have predominantly d character. However, the states at the ellipsoids have a substantial amount of s-p character. He argues that this s-p character makes these states less susceptible to defect scattering, as compared to states with pure d character. Thus the strength of oscillatory coupling associated with these parts of the Fermi surface is likely to be less reduced by defect scattering compared to those associated with other parts of the Fermi surface.

The calculated coupling strengths are much larger than values that have been measured.[6,8,13] This difference is not surprising, because interface roughness decreases the coupling strength of the long-period coupling as well as that of the short period, although by a different mechanism than that discussed in Sec. I. Diffuse scattering at the interfaces reduces the coherent reflection amplitude, reducing the coupling strength as in Eq. (2). Even the best Fe/Cr interfaces have a significant amount of interdiffusion.[30] Without knowing the detailed structure of the interfaces, and the scattering cross sections for interface defects, it is impossible to quantify the reduction in the coupling strength due to roughness.

IV. DISCUSSION

There have been several other proposed explanations for the origin of the long-period oscillatory coupling. These relate the origin of the coupling to other critical spanning vectors of the Cr Fermi surfaces. One interesting suggestion is that the long-period oscillation for the (001)-oriented films is due to aliasing of the second harmonic of the short-period oscillation.[15,31] Others suggested that the important critical spanning vectors are associated with the ''lens'' of the Fermi surface.[27,28] Another suggestion is that the long-period is due to a zone center spanning vector that is aliased by the antiferromagnetic order in the Cr.[17]

van Schilfgaarde and Harrison[31] have proposed that the long-period oscillation is due to the aliasing of the second harmonic of the short-period oscillation. This model makes the strong prediction that there is a definite relationship between the period of the two oscillations, $L_L = L_S/(2 - L_S)$. This predicted relationship appears to accurately describe the results of supercell calculations by vna Schilfgaarde et al.[15] However, it does not accurately describe experiment; it is inconsistent with the measured periods,[9] $L_L = 12 \pm 1$ ML and $L_S = 2.105 \pm 0.005$ ML.

TABLE II. Long-period contributions to the oscillatory exchange coupling. The position in the interface Brillouin zone is given by k_x and k_y. The periods are calculated within the local-density approximation (LDA), and for contributions from the N-centered ellipsoids, from fits to de Haas–van Alphen (dHvA) measurements of the Fermi surface. The coupling strengths, J^α are given as in Eq. (2).

Interface	k_x	k_y	Period LDA	Period dHvA	$J^\alpha/(1.0 \text{ nm})^2$
	(nm^{-1})	(nm^{-1})	(nm)	(nm)	(mJ/m^2)
Cr/Fe(100)	10.96	0.00	1.28	1.597	5.7
Cr/Fe(110)	0.00	15.50	1.47	1.816	3.2
	0.00	6.79	0.97		0.72
	9.89	0.00	0.94		0.91
Cr/Fe(112)	12.66	7.75	1.29	1.689	5.0
	5.56	6.73	1.15		2.8
	0.00	0.00	1.05		0.58

A possible reason for the discrepancy between the models that correctly describe the experiment and the supercell calculations is that the supercell calculations used Fe layers that were only two atomic layers thick. I find that the thinness of the Fe layers *decreases* the strength of the coupling due to the N-centered ellipsoids by a factor of 4, and *increases* that due to the aliasing of the second harmonic of the short period, also by a factor of 4. The coupling strengths change because the probability for Cr electrons to reflect from a finite thickness Fe layer embedded in bulk Cr depends on the thickness of the Fe. This dependence is illustrated in Fig. 4, which shows the reflection probability for the relevant states for various thicknesses of Fe. These reflection probabilities are not the total reflection probabilities, but the probabilities to reflect from a particular state into another particular state. The states chosen are the nested states along the $\overline{\Delta}$ line and the spanning vectors across the N-centered ellipsoid. Figure 4 shows that the reflection probabilities of the electrons at the critical point of the N-centered ellipsoids are reduced by a factor of 4 for reflection from two layers of Fe compared to that of bulk Fe. On the other hand, the reflection for the electrons from the ''nested'' regions of the Fermi surface is increased by a factor of 2. Since the strength of the coupling due to the second harmonic of the short-period oscillation is proportional to the square of this reflection probability, the strength of the coupling in the supercell calculation due to this mechanism is increased by a factor of 4, while the strength of the coupling due to the N-centered ellipsoids is reduced by a factor of 4. This change in relative strength by a factor of 16 gives a plausible explanation for the discrepancy between experiment and the supercell calculation.

The changes in reflection from finite thickness Fe layers are due to two different mechanisms as is illustrated in Fig. 4. The states on the N-centered ellipsoid reflect completely from an interface with bulk Fe, because there are no states in the Fe with the same symmetry. Only a fraction, 0.7, is reflected into the other side of the ellipsoid, while the rest is reflected into the jack and the other ellipsoid that projects to the same parallel wave vector. On the other hand, if the Fe layer has a finite thickness, electrons can tunnel through the Fe, reducing the reflection probability. The reflection mono-

tonically increases as the thickness of the Fe is increased. The Fe thickness dependence for the ''nested'' electrons is much more complicated. Here there are states of the same symmetry in the Fe, and the reflection is not complete even from bulk Fe. When the Fe layer has a finite thickness, there is multiple scattering from the two interfaces, giving a complicated interference pattern. For very thin Fe layers, this interference happens to increase the reflection probability. Thus, if the Fe layers can be grown thinly enough, and have both interfaces that are smooth enough, the coupling strength of the long-period oscillation should depend on the Fe layer thickness. The coupling due to the N-center ellipsoids will not change much except for the thinnest layers, but for these layers, the mechanism for the coupling might change to the aliasing of the second harmonic of the short-period (unless, of course, the Cr becomes antiferromagnetic under these conditions).

Fe/Cr superlattices grown with fixed Cr thickness show oscillatory properties as a function of Fe thickness.[32] These oscillations are indicative of oscillations in the exchange coupling that can arise from the type of interference found for the nested spanning vectors. The Cr thickness dependence of the coupling was not measured for these samples, so it is not known whether these oscillations are caused by the thickness dependence of the long-period oscillation, or whether there is some remnant of the short-period oscillation that has not been eliminated by the roughness of the interfaces. If the short-period oscillation can be described by the response of paramagnetic Cr, it would be expected to show strong oscillations with Fe thickness, based on the thickness dependence of the reflection probability.

Other proposals for the origin of the long-period oscillation are spanning vectors associated with the lens feature of the Fermi surface. The ''lens'' is a feature of the Cr Fermi surface that arises from the overlap of the octahedral feature at the center of the Brillouin zone and the ''knob'' feature near the middle of the Δ line (the feature associated by region B in Fig. 1). The resulting feature is centered at $k_{100}=7\,\text{nm}^{-1}$ and $k_{001}=0\,\text{nm}^{-1}$ in Fig. 1. In the plane shown in Fig. 1, the top and bottom of the lens have different symmetries, and hence meet at points. When spin-orbit coupling is included, these points become rounded. This region of the Fermi surface is of interest because in calculations of the Cr Fermi surface, based on the local-density approximation, the critical spanning vectors in this region have the periods closest to the experimentally measured period.[27,28] In the absence of spin-orbit coupling, the critical spanning vector is between states, with different symmetry.[27] The reflection probability, and hence coupling as in Eq. (2) between these two states, is strictly zero by symmetry. With spin-orbit coupling, the critical spanning vector is between states at the rounded tips of the lens.[28] While I have not computed the coupling associated with this spanning vector, it is likely to be quite weak because the radius of curvature at the the critical point κ_α will be small due to the weakness of spin-orbit coupling for first-row transition metals. In local density approximation calucations with spin-orbit coupling, Koelling[28] found small geometrical weights, $\propto v_\perp^\alpha \kappa^\alpha$ for all critical spanning in this region. Tsetseris, Lee, and Chang[18] computed the coupling strength as is done here, but included spin-orbit coupling in a tight-binding model of the band

structure. Because the geometrical weights are small, they found that the coupling due to the lens is quite small, as expected.

Recent photoemission experiments[22] purported to support the lens as the origin of the long-period oscillation. In a Cr overlayer on an Fe whisker substrate, Li *et al.* observed quantum-well states at the Fermi energy at a place in reciprocal space near the lens. As they varied the thickness of the overlayer, the states appeared at the Fermi level with a periodicity consistent with the period of the coupling observed in other experiments. While the existence of quantum well states is a necessary condition for long-range oscillatory coupling, it is not a sufficient one. It is necessary to establish that quantum-well states are at a critical point, which was not done in this experiment. In addition, to establish the origin of the long-period oscillation, it is necessary not only to show that it can be coming from one part of the Brillouin zone, but that it cannot be coming from other parts.

Figure 1 shows the Cr Fermi surface and highlights the spanning vectors relevant to this experiment. Li *et al.*[22] observed quantum-well states in the ''nested'' region, denoted by A, and in the jack near the lens, denoted by B. The results of the present paper suggest that the coupling is due to the N-centered ellipsoids, denoted by C. Figure 5 shows the state-to-state reflection probability and the period associated with all spanning vectors in Fig. 1. The spanning vectors labeled on the Fermi surface are circled in these panels. Strong reflection is found for the states in region B, where quantum-well states are found in the photoemission experiment, but at the critical points, the reflection becomes quite weak. Critical points occur wherever the period is constant as a function of parallel wave vector. These quantum-well states should exist for both majority and minority electrons. The phases of the reflection are sufficiently different for the different spins, so that the quantum-well states in a Cr layer surrounded by Fe should be almost completely out of phase with respect to each other. When one Cr/Fe interface is replaced by vacuum, this phase relationship will change. Quantum-well states are also seen experimentally at the Fermi energy in region A. The observation of these states at the Fermi energy suggests that the Cr is not antiferromagnetic, because these states are the part of the Fermi surface that disappears when Cr becomes antiferromagnetic.

Another proposed origin of the long-period oscillation is based on the analysis of electronic structure calculations for Cr embedded between two semi-infinite layers of Fe. Mirbt *et al.*[16] computed the coupling as a function of spacer thickness, and analyzed their results by fitting to a sum of 4 oscillatory terms. They attributed the long-period they extracted to a spanning vector at the center of the interface Brillouin zone. While I find coupling from several spanning vectors at the zone center, these spanning vectors all give short-periods, and have coupling strengths at least a factor of 5 weaker than that found for the N-centered ellipsoids. In this calculation, the periods are 0.24, 0.40, and 0.51 nm. Mirbt *et al.* invoked a doubling of the unit cell in the interface direction due to the antiferromagnetic state. With the longer unit cell, the 0.51 nm period is aliased to 1.67 nm (in the present calculation). However, the only experimental evidence available suggests that Cr is *not* in an antiferromagnetic state when the long-period oscillation is observed.[12] In

addition, the coupling is measured with each additional atomic layer, not with each additional doubled unit cell. This implies that the long-period found in the calculation has a different origin. The long-period found in the fit to the calculation could be due to the critical spanning vector across the N-centered ellipsoid. A possible explanation for any discrepancy between the extracted period and this spanning vector could be the susceptibility of the fit to the existence of many local minima.

V. SUMMARY

Calculations of the oscillatory coupling strength based on computing reflection probabilities at the critical points of the Fermi surface show that the long-period oscillation found in Fe/Cr multilayers is due to spanning vectors across the N-centered ellipsoids in the Cr Fermi surface. This conclusion holds for multilayers grown in the (001), (110), and (211) orientations. The measured periods disagree with those that are calculated using the local-density approximation, but agree with the periods extracted from the experimental Fermi surfaces.

[1] P. Grünberg, R. Schreiber, Y. Pang, M. B. Brodsky, and H. Sowers, Phys. Rev. Lett. **57**, 2442 (1986).

[2] M. N. Baibich, J. M. Broto, A. Fert, F. Nguyen Van Dau, F. Petroff, P. Etienne, G. Creuzet, A. Friederich, and J. Chazelas, Phys. Rev. Lett. **61**, 2472 (1988); G. Binasch, P. Grünberg, F. Saurenbach, and W. Zinn, Phys. Rev. B **39**, 4828 (1989).

[3] S. S. P. Parkin, N. More, and K. P. Roche, Phys. Rev. Lett. **64**, 2304 (1990).

[4] J. Unguris, R. J. Celotta, and D. T. Pierce, Phys. Rev. Lett. **67**, 140 (1991).

[5] S. T. Purcell, W. Folkerts, M. T. Johnson, N. W. E. McGee, K. Jager, J. aan de Stegge, W. B. Zeper, W. Hoving, and P. Grünberg, Phys. Rev. Lett. **67**, 903 (1991).

[6] S. Demokritov, J. A. Wolf, and P. Grünberg, Europhys. Lett. **15**, 881 (1991).

[7] For reviews of exchange coupling and GMR, including Fe/Cr multilayers, see A. Fert, P. Grünberg, A. Barthelemy, F. Petroff, and W. Zinn, J. Magn. Magn. Mater. **140-144**, 1 (1995); in *Ultrathin Magnetic Structures II,* edited by B. Heinrich and J. A. C. Bland (Springer-Verlag, Berlin, 1994), Chap. 2, p. 45.

[8] B. Heinrich and J. F. Cochran, Adv. Phys. **42**, 523 (1993).

[9] D. T. Pierce, J. A. Stroscio, J. Unguris, and R. J. Celotta, Phys. Rev. B **49**, 14 564 (1994).

[10] Y. Wang, P. M. Levy, and J. L. Fry, Phys. Rev. Lett. **65**, 2732 (1990).

[11] For a lengthy description of Cr and its antiferromagnetism, including illustrations of the Fermi surface, see E. Fawcett, Rev. Mod. Phys. **60**, 209 (1988).

[12] E. E. Fullerton, K. T. Riggs, C. H. Sowers, S. D. Bader, and A. Berger, Phys. Rev. Lett. **75**, 330 (1995).

[13] E. E. Fullerton, M. J. Conover, J. E. Mattson, C. H. Sowers, and S. D. Bader, Phys. Rev. B **48**, 15 755 (1993).

[14] M. van Schilfgaarde and F. Herman, Phys. Rev. Lett. **71**, 1923 (1993).

[15] M. van Schilfgaarde, F. Herman, S. S. P. Parkin, and J. Kudrnovský, Phys. Rev. Lett. **74**, 4063 (1995).

[16] S. Mirbt, H. L. Skriver, M. Alden, and B. Johansson, Solid State Commun. **88**, 331 (1993).

[17] S. Mirbt, A. M. N. Niklasson, B. Johansson, and H. L. Skriver, Phys. Rev. B **54**, 6382 (1996).

[18] L. Tsetseris, B. Lee, and Y.-C. Chang (unpublished).

[19] M. D. Stiles, J. Appl. Phys. **79**, 5805 (1996).

[20] For a calculation of the electronic structure of Cr/Fe superlattices and its effect on transport, see P. Zahn, I. Mertig, M. Richter, and H. Eschrig, Phys. Rev. Lett. **75**, 2996 (1995).

[21] J. E. Ortega, F. J. Himpsel, G. J. Mankey, and R. F. Willis, in *Magnetic Ultrathin Films: Multilayers and Surfaces, Interfaces and Characterization*, edited by B. T. Jonker *et al.* MRS Symposium Proceedings No. 313 (Materials Research Society, Pittsburgh, 1993), p. 143.

[22] D. Li, J. Pearson, S. D. Bader, E. Vescovo, D.-J. Huang, P. D. Johnson, and B. Heinrich (unpublished).

[23] M. D. Stiles and D. R. Hamann, Phys. Rev. B **38**, 2021 (1988); **40**, 1349 (1989).

[24] D. M. Edwards, J. Mathon, R. B. Muniz, and M. S. Phan, Phys. Rev. Lett. **67**, 493 (1991).

[25] P. Bruno and C. Chappert, Phys. Rev. Lett. **67**, 1602 (1991).

[26] P. Bruno, J. Magn. Magn. Mater. **121**, 238 (1993).

[27] M. D. Stiles, Phys. Rev. B **48**, 7238 (1993).

[28] D. D. Koelling, Phys. Rev. B **50**, 273 (1994).

[29] J. E. Graebner and J. A. Marcus, Phys. Rev. **175**, 659 (1968).

[30] D. Venus and B. Heinrich, Phys. Rev. B **53**, R1733 (1996); A. Davies, J. A. Stroscio, D. T. Pierce, and R. J. Celotta, Phys. Rev. Lett. **76**, 4175 (1996).

[31] M. van Schilfgaarde and W. A. Harrison, Phys. Rev. Lett. **71**, 3870 (1993).

[32] S. N. Okuno and K. Inomata, Phys. Rev. Lett. **72**, 1553 (1994).